


Genealogy of Leaky, Surface, and Plasmonic Modes in Partially Open Waveguides

Walter Fuscaldo^{1,*}, P. Burghignoli², and A. Galli²

¹Consiglio Nazionale delle Ricerche Istituto per la Microelettronica e Microsistemi, Rome, Italy

²Sapienza University of Rome Department of Information Engineering, Electronics and Telecommunications, Rome, Italy

 (Received 6 August 2021; revised 3 February 2022; accepted 11 February 2022; published 14 March 2022)

The presence of a partially reflecting screen on top of a grounded dielectric slab strongly perturbs its modal spectrum. The modes supported by such structures have been investigated in the literature for some specific, yet relevant cases. Here, a comprehensive modal analysis is presented, which emphasizes the inductive or capacitive nature of the partially reflecting sheet. The results of this analysis not only provide a clear overview of a wide class of structures of relevance in applied electromagnetics, but also unveil the presence of some useful propagating regimes so far barely explored.

DOI: [10.1103/PhysRevApplied.17.034038](https://doi.org/10.1103/PhysRevApplied.17.034038)

I. INTRODUCTION

In electromagnetics as in acoustics, systems exhibiting parity-time symmetries [1,2] support symmetry-protected, bounded-in-continuum states that allow for the propagation of localized, self-trapped modes [3]. The quest for such topologically protected states has led to the discovery of unique propagation regimes, such as *soleakons* [4], i.e., solitonlike solutions that interact with each other through continuum (as *leaky waves*), *line waves* [5,6], i.e., the one-dimensional version of surface plasmon polaritons, topological edge modes [7], exceptional points of degeneracy [8], just to name but a few. In order to show these properties, the structures usually exhibit peculiar symmetries, such as positive or negative nonlinearities [4], non-Hermitian metasurfaces [5], perfect electrically and magnetically conducting waveguides [7]. However, even simpler structures such as planar metallic-dielectric ones may support unusual propagation regimes.

Planar metallic-dielectric structures are the basic constituents of several electromagnetic waveguiding and radiating devices; in particular, the grounded dielectric slab, Fig. 1(a) and the parallel-plate waveguide, Fig. 1(c) are two canonical examples of *open* and *closed* structure [9, 10]. The modal spectra of these two configurations are well known. Assuming lossless media, parallel-plate waveguides support either *guided waves*, with a real wave number, or *evanescent waves*, with a purely imaginary wave number. Grounded dielectric slabs, on the other hand, support either *surface waves*, with a real wave number, or *leaky waves*, with a complex wave number that accounts for radiation losses. As in any open waveguide, a further classification can be based on the behavior of the modal

fields at infinity in the transverse direction: if the Sommerfeld radiation condition is satisfied, modes are said to be *proper*, conversely they are *improper*; if the substrate is an ordinary dielectric medium, then surface waves can be either proper (i.e., *bound* to the substrate) or improper (i.e., *unbounded*), whereas leaky waves are always improper (unless they are *backward leaky waves*).

When a partially reflecting sheet or screen is placed on top of the grounded dielectric slab, thus obtaining a *loaded* grounded dielectric slab [see Fig. 1(b)], plasmonic waves may appear at the air-dielectric interface providing tightly confined propagation regimes, and leaky waves may become weakly attenuated [10–12] providing highly directive radiation regimes [13,14]. Therefore, the presence of a partially reflecting sheet on top of a grounded dielectric slab strongly perturbs its modal spectrum and in turn the fundamental electromagnetic properties of the structure. Practical realizations of partially reflecting screens can be, e.g., uniform dielectric superstrates with high permittivity, distributed Bragg reflectors, or thin periodic patterned metal sheets such as arrays of rectangular patches or slots etched in a uniform metal plate [13]. It is worthwhile to stress that, in the latter case, we consider those patterns that are subwavelength and act as a homogeneous, isotropic, metasurface [15]. Although the results reported here apply even to more general cases, the previous assumption allows us to describe the partially reflecting screen with a single scalar impedance, thus providing a great simplification of the problem while keeping sufficient generality.

The *complex* modal spectrum of grounded dielectric slabs characterized by ferrite layers, anisotropic and bianisotropic materials, has also been widely investigated [16,17], whereas the specific properties of leaky waves in several classes of both open and closed planar structures

*walter.fuscaldo@cnr.it

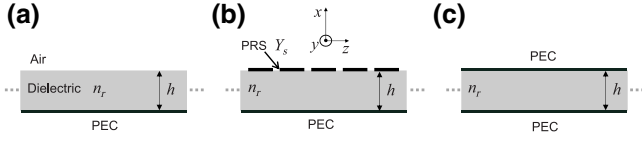


FIG. 1. Cross section of the three reference structures considered here: (a) a grounded dielectric slab; (b) a grounded dielectric slab loaded by a partially reflecting screen (PRS); (c) a parallel-plate waveguide. The acronym PEC stands for perfect electric conductor.

have been discussed in Refs. [18–20]. The modal spectrum of the loaded grounded dielectric slab [see Fig. 1(b)] has been investigated only for certain specific cases, e.g., in Refs. [21–24] when the sheet is made of graphene, or in Ref. [25] when a capacitive sheet is employed. Recently, the effects of the juxtaposition of an inductive sheet side by side with a capacitive sheet revealed the existence of *line waves* [5,6]. On the other hand, a comprehensive and systematic study of the entire complex modal spectrum of a loaded grounded dielectric slab distinguishing between the inductive and capacitive nature of the whole partially reflecting sheet and the transverse electric (TE) and transverse magnetic (TM) nature of surface, leaky, and plasmonic waves is still lacking.

In this work, we show that even the introduction of a simple partially reflecting sheet made, e.g., from a thin periodic metal sheet [see Fig. 1(b)] in a grounded dielectric slab gives rise to a number of intriguing physical phenomena. In particular, it turns out that the inductive or capacitive character of the partially reflecting sheet plays a key role in determining the physical properties of the complex modal spectrum.

An accurate characterization of the latter is crucial in a number of applications in both physics and engineering. For instance, leaky modes are typically employed for the design of traveling-wave radiators with frequency scannable or shaped radiation patterns, operating at frequencies from the microwave range to millimeter-wave, terahertz, and optical ranges [13]. A more recent and peculiar application of leaky modes is related to the realization of resonant waveguides capable of focusing radiation in the form of *Bessel beams* in the radiative near field (see, e.g., Ref. [26]). The limited-diffraction, self-healing, and (for higher-order) orbital angular momentum transport properties of Bessel beams find application in various contexts, spanning from micromanipulation of particles and medical imaging in optical ranges [27–30], to wireless power and information transfer at lower frequencies [25,31,32].

II. MODAL SPECTRUM OF OPEN AND CLOSED WAVEGUIDES

An idea of the complexity of this perturbation can be inferred from Fig. 2, where it is shown how the modal

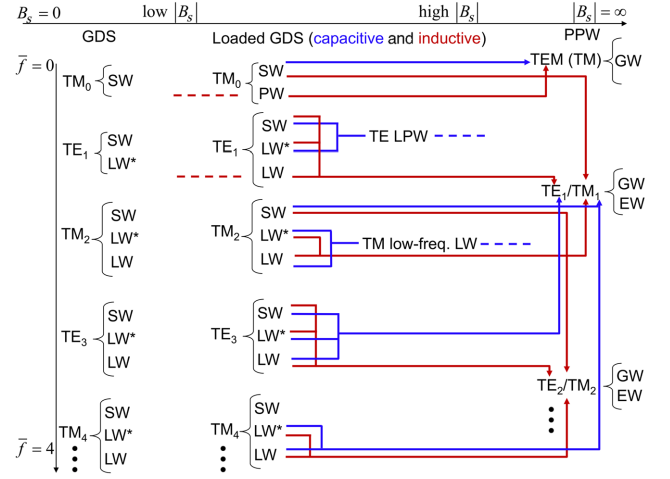


FIG. 2. Genealogy of the modes supported by a grounded dielectric slab (GDS) loaded by an inductive and capacitive partially reflecting screen or sheet (PRS). Dashed lines are used for modes that no longer exist for the asymptotic cases $B_s \rightarrow 0, \infty$. The following acronyms are used: parallel-plate waveguide (PPW), surface wave (SW), leaky wave (LW), plasmonic wave (PW), leaky plasmonic wave (LPW), guided wave (GW), evanescent wave (EW). The asterisk “*” after “LW” is used to highlight the *nonphysical* nature of such a leaky wave, as commented in the text.

spectrum of a grounded dielectric slab turns in a different way into that of a parallel-plate waveguide as the reflectivity of the partially reflecting sheet increases (moving from left to right) to equate that of a perfect electric conductor depending on whether a capacitive sheet (blue lines) or an inductive sheet (red lines) is used.

The previous findings and other results are manifest from a rigorous modal analysis of the structures. Without loss of generality, in the following we consider the substrate made of a lossless dielectric with refractive index $n_r = 1.45$ and a lossless partially reflecting sheet described by a single, scalar, sheet susceptance B_s that fully characterizes its electromagnetic properties (this description proves to be accurate for a wide class of metallic sheet in the homogenization limit, i.e., with subwavelength periodic features [15]). The structure is supposed to be of infinite extent in the transverse direction (y - z plane in Fig. 1) and invariant along the y axis, thus the dispersion equations can easily be derived from a standard application of the field-matching technique [33] (a time-harmonic dependence $e^{j\omega t}$ is assumed):

$$\text{(TE)} : \hat{k}_{x0} + j\bar{B}_s - j\hat{k}_{xd} \cot(k_0\hat{k}_{xd}h) = 0, \quad (1a)$$

$$\text{(TM)} : \hat{k}_{x0}^{-1} + j\bar{B}_s - jn_r^2\hat{k}_{xd}^{-1} \cot(k_0\hat{k}_{xd}h) = 0, \quad (1b)$$

where $\hat{k}_{x0} = \sqrt{1 - \hat{k}_z^2}$ and $\hat{k}_{xd} = \sqrt{n_r^2 - \hat{k}_z^2}$ are the normalized vertical wave number in vacuum and in the dielectric,

respectively, and $\hat{k}_z = \hat{\beta} - j\hat{\alpha}$ is the normalized longitudinal propagation wave number. The “bar” and the “hat” refers to normalization with respect to the vacuum impedance $\eta_0 \simeq 120\pi \Omega$, and wave number $k_0 = 2\pi/\lambda$ (λ being the vacuum wavelength), respectively.

We recall that the domain of the functions at the left-hand sides of Eqs. (1a)–(1b) is a two-sheeted Riemann surface, the proper $\text{Im}\{k_x\} < 0$ and improper $\text{Im}\{k_x\} > 0$ sheets being connected through the Sommerfeld branch cuts $\text{Im}\{k_x\} = 0$ [11]; we represent the trajectories of proper modes (such as guided, evanescent, surface, and plasmonic waves) with solid lines, and those of improper modes (such as leaky waves) with dashed or dotted lines. As is well known [33], in addition to the TE and TM guided and evanescent waves, the parallel-plate waveguide modal spectrum accounts for a nondispersive TEM guided mode with $\hat{k}_z = n_r$ as a consequence of the nonconnected topology of the structure.

The grounded dielectric slab and the parallel-plate waveguide can be obtained as asymptotic cases for $|\bar{B}_s| \rightarrow 0$ and $|\bar{B}_s| \rightarrow \infty$, respectively. The thickness of the dielectric slab is equal to $h = \lambda_0/2n_r$, where λ_0 is the vacuum wavelength at the reference frequency f_0 (as in Fabry–Perot-cavity structures), f_0 being the cutoff frequency of the first TM_1 and TE_1 guided modes’ degenerate pair, i.e., the frequency at which $\beta = 0$ in the parallel-plate waveguide.

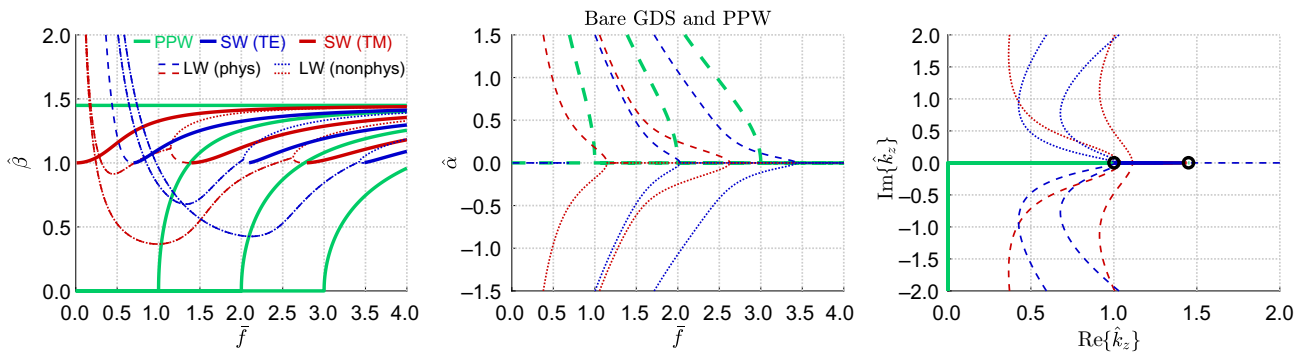
The dispersion diagrams of the parallel-plate waveguide modes in both the guided-wave and the evanescent-wave regimes (along with those supported by the grounded dielectric slab, as we soon comment) are obtained from the well-known analytic formula $\hat{k}_{zn} = n_r \sqrt{1 - (nf_0/f)^2}$, $n \in \mathbb{N}$ and are reported in Video 1 as $\hat{\beta}$ vs $\bar{f} = f/f_0$ (left, guided waves in solid green lines), $\hat{\alpha}$ vs \bar{f} (center, evanescent in dashed green lines), and as trajectories in the complex \hat{k}_z plane (right, solid green lines).

On the other hand, a grounded dielectric slab supports TE and TM surface waves that have an analytic (complex)

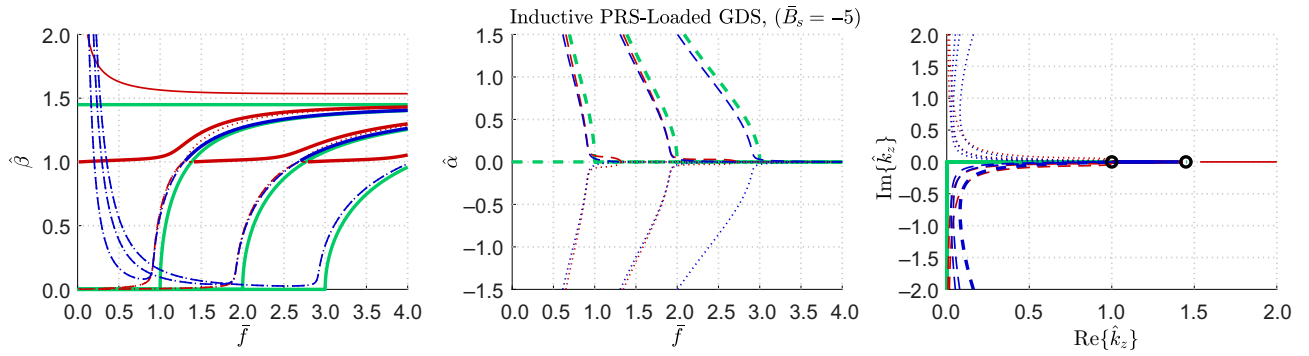
continuation below the surface-wave cutoff (i.e., the frequency for which $\beta = k_0$), commonly known as leaky waves. These leaky waves possess a quadrantal symmetry with respect to the origin of the complex k_z plane [11] (for lossless media), but we consider only the complex conjugate pair with $\hat{\beta} > 0$: the improper, yet *physical* (i.e., with $\hat{\alpha} > 0$) solutions, labeled as LW in Fig. 2 and reported with dashed lines, and the improper, *nonphysical* solutions (i.e., with $\hat{\alpha} < 0$) labeled as LW* in Fig. 2 and reported with dotted lines. Exceptions to this symmetry are the TM_0 surface wave, which has no cutoff, and hence no analytic continuation, and the TE_1 surface wave (as is customary [33], we index TM and TE surface waves with an even or odd number, respectively), which only has a real improper surface-wave mode. All higher-order TE and TM surface waves have instead a pair of physical and nonphysical leaky modes modes. With an abuse of notation, real improper surface-wave modes are still labeled as LW* and thus reported with dotted lines as well.

The dispersion curves of TE_{2n+1} and TM_{2n} , surface-wave modes are obtained by solving for the roots of the dispersion Eqs. (1a)–(1b) (see, e.g., Ref. [34]) and are reported in Video 1 in solid blue and red lines, respectively, whereas their analytical continuations, i.e., the physical and nonphysical leaky-wave complex conjugate pair, are reported in dashed and dotted lines for both the TE (in blue) and TM (in red) cases.

We recall here the typical evolution of the leaky-wave complex conjugate pair into surface-wave modes as the frequency increases. As is known [16], the physical and the nonphysical leaky modes coalesce at the *splitting point* where they enter the so-called *spectral gap*: a frequency region where the *improper* leaky complex conjugate pair turns into a pair of *improper* surface waves characterized by a purely real wave number. As the frequency increases, one of these improper surface waves (the real improper surface wave that we refer to as LW* and thus represent with a dotted line) proceeds its trajectory over the improper Riemann sheet, whereas the other one “jumps” through



VIDEO 1. Dispersion diagrams of the modes supported by two canonical open and closed structures: the grounded dielectric slab (GDS) and the parallel-plate waveguide (PPW), respectively. (Left) $\hat{\beta}$ vs \bar{f} , (center) $\hat{\alpha}$ vs \bar{f} , and (right) $\text{Im}\{\hat{k}_z\}$ vs $\text{Re}\{\hat{k}_z\}$. The acronyms used in this figure are defined in the captions of Figs. 1 and 2.



VIDEO 2. As in Video 1, but for an inductivelike loaded GDS.

the branch points at $\pm k_0$ into the proper Riemann sheet and gives rise to a *proper* surface wave as the frequency goes beyond the corresponding surface wave cutoff. An animation that shows the frequency evolution of the complex modal spectra of the parallel-plate waveguide and the grounded dielectric slab is available upon clicking on Video 1. From this animation, one can better appreciate the evolution of the entire complex modal spectrum of a grounded dielectric slab and a parallel-plate waveguide. In this regard it is also worth noting the *pole crowding* at $\hat{k}_z = n_r$, experienced by all surface-wave modes at frequencies considerably above their cutoffs.

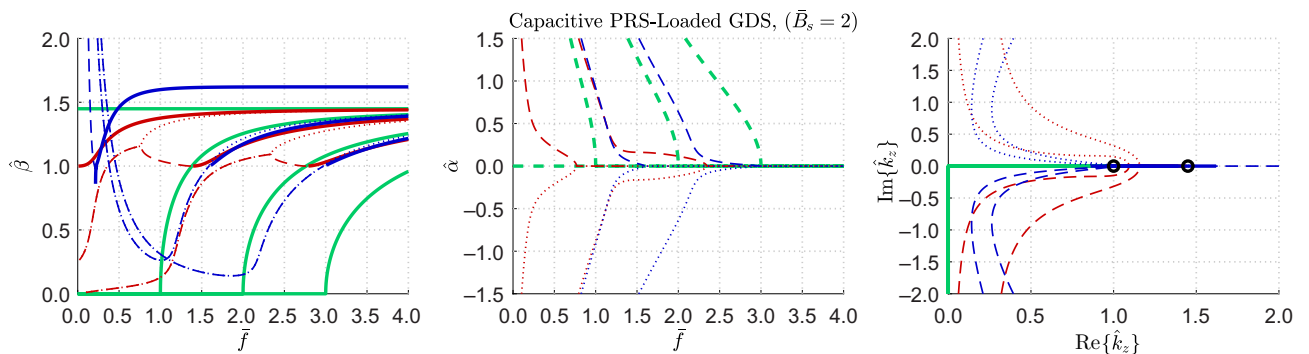
III. GENEALOGY OF THE MODES IN A PARTIALLY OPEN WAVEGUIDE

At this point we can introduce the partially reflecting sheet and see how the modal spectrum of a grounded dielectric slab transitions into the modal spectrum of a parallel-plate waveguide. We should distinguish the effects of the inductive ($\bar{B}_s < 0$) or the capacitive nature ($\bar{B}_s > 0$) of the sheet as well as the TE or the TM nature of the modes. Therefore, we have four different cases that are worth investigating separately. In all cases, the values provided for \bar{B}_s are referred to as the value assumed by the normalized sheet susceptance at $\bar{f} = 1$; for $\bar{f} \neq 1$, \bar{B}_s is modeled with a capacitivelike or inductivelike dispersive

behavior depending on the sign of \bar{B}_s . As for Video 1, an animation that shows the frequency evolution of the complex modal spectra of these two structures is available upon clicking on Videos 2 and 3 for the inductive and the capacitive cases, respectively.

A. TM modes: inductive case

We start by analyzing the effects of an inductive sheet with $\bar{B}_s = -5$ on the TM modes (see red curves in Video 2). Different choices of the \bar{B}_s value would give different results, but would lead to the same conclusion; the choice made here allows only for having a clear distinction from the two asymptotic cases (viz., the grounded dielectric slab and the parallel-plate waveguide). From Video 2 we see that the use of an inductive sheet introduces a TM plasmonic wave that asymptotically converges to the TEM guided mode of a parallel-plate waveguide as the sheet turns into a perfect electric conductor. This effect can be easily predicted from the approximate dispersion equation of a TM plasmonic wave supported by an inductive sheet, which reads $\hat{k}_z = n_{\text{eff}} \sqrt{1 + (2n_{\text{eff}}/\bar{B}_s)^2}$, where $n_{\text{eff}} \simeq \sqrt{(n_r^2 + 1)/2}$ is the effective refractive index. (Note that the tight field confinement of plasmonic waves allows for ignoring the presence of the ground plane, and thus safely using the previous dispersion equation.) Therefore,



VIDEO 3. As in Video 1, but for a capacitivelike loaded GDS.

if $\bar{B}_s \rightarrow -\infty$ then $\hat{k}_z \rightarrow n_{\text{eff}}$, whereas, for $\bar{B}_s \rightarrow 0^-$, $\hat{k}_z \rightarrow \infty$, hence the TM plasmonic wave becomes extremely slow and eventually vanishes. The dispersion curve of the plasmonic wave is represented with a thin solid red curve with $\hat{\beta} > n_r$, as is manifest from Video 2 (left). From Video 2 (left) we can also appreciate another effect of the inductive sheet perturbation: the dispersion curves of both the TM_{2n} leaky waves and the TM_{2n-2} surface waves “bend” towards higher frequencies to recover the dispersion curve of the parallel-plate waveguide TM_n guided and evanescent waves. More precisely, it is noted that, as $|B_s|$ increases, the cutoff frequencies of TM surface waves remain fixed, but the *leaky* cutoff frequencies of TM leaky waves blueshift, i.e., they increase. (We recall here that leaky-wave cutoffs correspond to the condition $\hat{\beta} = \hat{\alpha}$.) As a result, the spectral-gap region narrows and tends to disappear as the sheet becomes a perfect electric conductor. The *contraction* of the spectral gap as the sheet becomes more reflective is also shown by TE modes in both the inductive and the capacitive case, but not by TM modes in the capacitive case as we soon comment.

B. TE modes: inductive case

In the TE case [see blue curves in Video 2 (left)], as opposed to the TM case, the surface-wave cutoffs do not remain fixed, but blueshift [cf. blue solid curves in Video 2 (left) with those in Video 1 (left)]: the net effect is that TE leaky and surface waves experience a “rigid” translation towards higher frequencies as $|B_s|$ increases. For $B_s \rightarrow -\infty$, the TE_{2n-1} , $n \geq 1$ surface and leaky waves asymptotically recover the parallel-plate waveguide TE_n guided and evanescent waves. Even more interestingly, a TE_1 leaky mode appears to reconstitute the TE_1 physical and nonphysical leaky complex conjugate pair (that in a grounded dielectric slab is *orphan* of the *physical* leaky-wave solution). Such TE_1 physical leaky mode, for the high value of B_s chosen here, becomes fast and thus can profitably be used for radiation (as has been done, e.g., in Ref. [22]). As for the TM case, the spectral-gap region narrows as $|B_s|$ increases.

C. TM modes: capacitive case

We now analyze the effects of a capacitive sheet with $\bar{B}_s = 2$, on the TM modes first (see red curves in Video 3). In this case we do not have a plasmonic wave, but it is the TM_0 surface wave that asymptotically recovers the TEM guided mode of the parallel-plate waveguide for $B_s \rightarrow +\infty$. In general, and in contrast with the inductive case, as $|B_s|$ increases the TM surface-wave dispersion curves “bend” towards lower frequencies, whereas the leaky-wave cutoffs redshift, i.e., they decrease [cf. red dashed curves in Video 3 (left) with those in Video 1 (left)]. Since the TM surface-wave cutoffs remain fixed,

the spectral-gap region stretches out as $B_s \rightarrow +\infty$ [(compare the dashed red curves of Video 3 with those of Video 2)]. This is a remarkable aspect that distinguishes the behavior of TE and TM modes in capacitivelike loaded grounded dielectric slabs from that shown in inductive-like loaded grounded dielectric slabs that we previously commented. Moreover, the TM_{2n} , $n \geq 1$ surface waves and TM_{2n+2} leaky waves asymptotically recover the parallel-plate waveguide TM_n guided and evanescent waves for $B_s \rightarrow +\infty$. Evidently, the TM_2 leaky wave vanishes for $B_s \rightarrow +\infty$ since the fundamental parallel-plate waveguide TEM mode has no cutoff, thus no analytic continuation. In this regard, it is worthwhile to stress that for large values of $|B_s|$ the TM_2 leaky-wave mode becomes a low-frequency mode that is in fact profitably used to design radiating devices characterized by ultrasubwavelength substrate thickness (see, e.g., Refs. [25,32,35]). This is a key feature of TM modes in capacitivelike loaded grounded dielectric slab: in other cases, it is never possible to have radiation from the electrically thin-loaded grounded dielectric slab using forward leaky-wave modes and a simple, isotropic partially reflecting sheet.

D. TE modes: capacitive case

In the TE case (see blue curves in Video 3), both surface- and leaky-wave cutoffs redshift [cf. blue curves in Video 3 (left) with those in Video 1 (left)]. Consequently, TE_{2n+1} , $n \geq 1$ surface waves and leaky waves asymptotically recover parallel-plate waveguide TE_n guided and evanescent waves for $B_s \rightarrow +\infty$. Here, the “rigid” frequency redshift of the modes narrows the spectral-gap region as $B_s \rightarrow +\infty$, as it occurs for both TE and TM modes in the inductive case. Specific attention is given to the TE_1 surface wave for which only an improper real surface wave exists, not the entire leaky complex conjugate pair is deserved. Indeed, a capacitive sheet supports a TE plasmonic wave and since there is no TE mode in a loaded grounded dielectric slab that asymptotically converges to the TEM guided mode of a parallel-plate waveguide, this TE plasmonic wave turns into the TE_1 surface wave for $B_s \rightarrow 0^+$. As for the TM case, this effect can be easily predicted from the approximate dispersion equation of TE plasmonic waves, which reads $\hat{k}_z = \sqrt{n_{\text{eff}}^2 + (\bar{B}_s/2)^2}$. In this case, there might exist frequency ranges for which $1 < \hat{\beta} < n_r$, and even $\hat{\beta} < 1$. In open structures, such TE plasmonic waves are said *leaky plasmonic waves* as they may “leak” some energy into the substrate or even radiate into space [20,36]. Interestingly, this happens to be the case even in partially open structures such as the grounded dielectric slab loaded with a capacitive sheet considered here, where there exist, in fact, narrow frequency ranges for which $\hat{\beta} < 1$ [its “leakage” into the $\hat{\beta} < 1$ region is also appreciable in Video 3

(left)]. As opposed to the TM plasmonic wave, the TE *leaky plasmonic* wave vanishes for $\bar{B}_s \rightarrow +\infty$, whereas for $\bar{B}_s \rightarrow 0$, it transitions into the TE surface wave. One might be tempted to conclude that, in capacitivelike loaded grounded dielectric slab, TE plasmonic wave and TE₁ surface waves are two sides of the same coin: the former appearing for high \bar{B}_s , the latter appearing for low \bar{B}_s .

IV. CONCLUSION

To conclude, we see that although intriguing propagating regimes are currently being discovered by conceptualizing more and more elaborated structures, or breaking either geometrical or electromagnetic symmetries, a simple planar metallic-dielectric structure with a single dielectric layer and, e.g., a patterned metallic layer opens to a number of unusual properties so far barely explored. TE leaky plasmonic waves and low-frequency TM leaky-wave modes are but two relevant examples. In the future, it would be useful to extend such a systematic analysis and genealogy of modes to more complicated three-dimensional structures, such as those supporting line waves [5], as well as to nonidealities of the partially reflecting sheet (effects of losses [37], tensorial formulations [38], etc.) and metamaterials [39].

-
- [1] C. M. Bender and S. Boettcher, Real Spectra in Non-Hermitian Hamiltonians Having \mathcal{PT} Symmetry, *Phys. Rev. Lett.* **80**, 5243 (1998).
- [2] S. Malzard, C. Poli, and H. Schomerus, Topologically Protected Defect States in Open Photonic Systems with Non-Hermitian Charge-Conjugation and Parity-Time Symmetry, *Phys. Rev. Lett.* **115**, 200402 (2015).
- [3] C. W. Hsu, B. Zhen, A. D. Stone, J. D. Joannopoulos, and M. Soljačić, Bound states in the continuum, *Nat. Rev. Mat.* **1**, 1 (2016).
- [4] O. Peleg, Y. Plotnik, N. Moiseyev, O. Cohen, and M. Segev, Self-trapped leaky waves and their interactions, *Phys. Rev. A* **80**, 041801(R) (2009).
- [5] M. Moccia, G. Castaldi, A. Alù, and V. Galdi, Line waves in non-Hermitian metasurfaces, *ACS Photonics* **7**, 2064 (2020).
- [6] D. J. Bisharat and D. F. Sievenpiper, Guiding Waves along an Infinitesimal Line between Impedance Surfaces, *Phys. Rev. Lett.* **119**, 106802 (2017).
- [7] E. Martini, M. G. Silveirinha, and S. Maci, Exact solution for the protected TEM edge mode in a PTD-symmetric parallel-plate waveguide, *IEEE Trans. Antennas Propag.* **67**, 1035 (2018).
- [8] M. A. K. Othman, V. Galdi, and F. Capolino, Exceptional points of degeneracy and \mathcal{PT} symmetry in photonic coupled chains of scatterers, *Phys. Rev. B* **95**, 104305 (2017).
- [9] G. W. Hanson and A. B. Yakovlev, *Operator Theory for Electromagnetics* (Springer, Heidelberg, Germany, 2013).
- [10] N. Marcuvitz, On field representations in terms of leaky modes or eigenmodes, *IRE Trans. Antennas Propag.* **4**, 192 (1956).
- [11] T. Tamir and A. A. Oliner, Guided complex waves. Part 1: Fields at an interface, *Proc. IEE* **110**, 310 (1963).
- [12] T. Tamir and A. A. Oliner, Guided complex waves. Part 2: Relation to radiation patterns, *Proc. IEE* **110**, 325 (1963).
- [13] D. R. Jackson, P. Burghignoli, G. Lovat, F. Capolino, J. Chen, D. R. Wilton, and A. A. Oliner, The fundamental physics of directive beaming at microwave and optical frequencies and the role of leaky waves, *Proc. IEEE* **99**, 1780 (2011).
- [14] D. R. Jackson, C. Caloz, and T. Itoh, Leaky-wave antennas, *Proc. IEEE* **100**, 2194 (2012).
- [15] S. Tretyakov, *Analytical Modeling in Applied Electromagnetics* (Artech House, Norwood, MA, USA, 2003).
- [16] A. B. Yakovlev and G. W. Hanson, Fundamental modal phenomena on isotropic and anisotropic planar slab dielectric waveguides, *IEEE Trans. Antennas Propag.* **51**, 888 (2003).
- [17] A. B. Yakovlev and G. W. Hanson, Leaky-wave dispersion behavior on a grounded ferrite slab waveguide, *IEEE Microw. Wireless Comp. Lett.* **12**, 398 (2002).
- [18] G. W. Hanson and A. B. Yakovlev, An analysis of leaky-wave dispersion phenomena in the vicinity of cutoff using complex frequency plane singularities, *Radio Sci.* **33**, 803 (1998).
- [19] A. B. Yakovlev and G. W. Hanson, On the nature of critical points in leakage regimes of a conductor-backed coplanar strip line, *IEEE Trans. Microw. Theory Tech.* **45**, 87 (1997).
- [20] J. J. Burke, G. I. Stegeman, and T. Tamir, Surface-polariton-like waves guided by thin, lossy metal films, *Phys. Rev. B* **33**, 5186 (1986).
- [21] G. W. Hanson, Dyadic Green's functions and guided surface waves for a surface conductivity model of graphene, *J. Appl. Phys.* **103**, 064302 (2008).
- [22] W. Fuscaldo, P. Burghignoli, P. Baccarelli, and A. Galli, Complex mode spectra of graphene-based planar structures for THz applications, *J. Infrared Milli. Terahz Waves* **36**, 720 (2015).
- [23] A. Vakil and N. Engheta, Transformation optics using graphene, *Science* **332**, 1291 (2011).
- [24] A. Vakil and N. Engheta, Fourier optics on graphene, *Phys. Rev. B* **85**, 075434 (2012).
- [25] W. Fuscaldo, G. Valerio, A. Galli, R. Sauleau, A. Grbic, and M. Ettore, Higher-order leaky-mode Bessel-beam launcher, *IEEE Trans. Antennas Propag.* **64**, 904 (2016).
- [26] M. Ettore, S. C. Pavone, M. Casaletti, M. Albani, A. Mazzinghi, and A. Freni, in *Aperture Antennas for Millimeter and Sub-Millimeter Wave Applications* (Springer, Cham, Switzerland, 2018), p. 243.
- [27] M. Ormigotti, C. Conti, and A. Szameit, Effect of Orbital Angular Momentum on Nondiffracting Ultrashort Optical Pulses, *Phys. Rev. Lett.* **115**, 100401 (2015).
- [28] K. Volke-Sepulveda, V. Garcés-Chávez, S. Chávez-Cerda, J. Arlt, and K. Dholakia, Orbital angular momentum of a high-order Bessel light beam, *J. Opt. B: Quantum Semi-classical Opt.* **4**, S82 (2002).
- [29] A. M. Yao and M. J. Padgett, Orbital angular momentum: Origins, behavior and applications, *Adv. Opt. Photonics* **3**, 161 (2011).

- [30] D. McGloin and K. Dholakia, Bessel beams: Diffraction in a new light, *Contemporary Phys.* **46**, 15 (2005).
- [31] A. Grbic, L. Jiang, and R. Merlin, Near-field plates: Sub-diffraction focusing with patterned surfaces, *Science* **320**, 511 (2008).
- [32] J. D. Heeb, M. Ettore, and A. Grbic, Wireless Links in the Radiative near Field via Bessel Beams, *Phys. Rev. Appl.* **6**, 034018 (2016).
- [33] R. E. Collin, *Field Theory of Guided Waves* (IEEE Press, New York, NY, USA, 1991), 2nd ed.
- [34] V. Galdi and I. M. Pinto, A simple algorithm for accurate location of leaky-wave poles for grounded inhomogeneous dielectric slabs, *Microw. Opt. Technol. Lett.* **24**, 135 (2000).
- [35] M. Ettore and A. Grbic, Generation of propagating Bessel beams using leaky-wave modes, *IEEE Trans. Antennas Propag.* **60**, 3605 (2012).
- [36] S. A. Maier, *Plasmonics: Fundamentals and Applications* (Springer, New York, NY, USA, 2007).
- [37] W. Fuscaldo, Rigorous evaluation of losses in uniform leaky-wave antennas, *IEEE Trans. Antennas Propag.* **68**, 643 (2020).
- [38] K. Achouri and C. Caloz, Design, concepts, and applications of electromagnetic metasurfaces, *Nanophotonics* **7**, 1095 (2018).
- [39] N. Engheta and R. W. Ziolkowski, *Metamaterials: Physics and Engineering Explorations* (John Wiley & Sons, Hoboken, NJ, USA, 2006).